

proteins appear to be paralogs that arose by a gene duplication in Eukarya. The GenBank accession numbers for the aNOP56 and aFIB protein sequences from *S. acidocaldarius* are AF201092 and AF201093, respectively.

8. J. R. Chamberlain, Y. Lee, W. S. Lane, D. R. Engelke, *Genes Dev.* **12**, 1678 (1998).
9. P. Wu, J. S. Brockenbrough, A. C. Metcalfe, S. Chen, J. P. Aris, *J. Biol. Chem.* **273**, 16453 (1998). Briefly, the primer AO30 (5'-CTCAGATCTGGATCCGGG-3') was 5' phosphorylated with T4 polynucleotide kinase and adenosine triphosphate (ATP) and blocked at the 3' end with terminal deoxynucleotidyl transferase (Gibco BRL) and dideoxycytidine triphosphate (ddCTP). The modified oligo was then ligated to gel-purified sRNA for 16 hours at 4°C. The ligation products were reverse transcribed with Thermoscript RT (Gibco BRL) at 55°C for 30 min, with AO31 (5'-CCCGATCCAGATCTCGAG-3') as primer. The RNA template was hydrolyzed with ribonuclease H, and the cDNA strand was extended with deoxy-ATP with terminal deoxynucleotidyl transferase. The extended cDNA strand was used as template for PCR (95°C denaturation, 65°C hybridization, 72°C extension, 30 cycles) with AO31 and AO32 [5'-GCGAAT-TCTGCAG(T)<sub>30</sub>-3'] as primers. The DNA products were cleaved with Pst I and Xho I, ligated between the Pst I and Xho I sites of plasmid pSP72, and transformed into *E. coli*. Plasmids were isolated and their sequences were determined.
10. Z. Kiss-Laszlo, Y. Henry, T. Kiss, *EMBO J.* **17**, 797 (1998).
11. Southern hybridizations confirmed the existence of single-copy genes for sR1, sR2, sR5, and sR13 in *S. acidocaldarius* genomic DNA. Genomic clones of the *S. acidocaldarius* sR1 and *S. solfataricus* sR1 were isolated and sequenced. In both cases, the sRNA genes overlap the 3' end of the corresponding aspartate aminotransferase genes. The translation termination codons UAA for *S. acidocaldarius* and UAG for *S. solfataricus* fall within the D' box guide regions in the two sRNAs (Fig. 4A).
12. S. F. Altschul *et al.*, *Nucleic Acids Res.* **25**, 3389 (1997). The BLAST searches against the nonredundant nucleotide database were performed at [www.ncbi.nlm.nih.gov/BLAST/](http://www.ncbi.nlm.nih.gov/BLAST/) on 15 June 1999.
13. G. J. Olsen *et al.*, *J. Mol. Evol.* **22**, 301 (1985); D. A. Stahl, K. R. Luehrsen, C. R. Woese, N. R. Pace, *Nucleic Acids Res.* **9**, 6129 (1981); E. Dams, P. Londei, P. Cammarano, A. Vandenbergh, R. De Wachter, *Nucleic Acids Res.* **11**, 4667 (1983); P. Durovic and P. P. Dennis, *Mol. Microbiol.* **13**, 229 (1994). As a result of strain misidentification, the 16S RNA sequence published in the first paper is now recognized to be from *S. acidocaldarius* and not *S. solfataricus* as originally indicated. The two originally published 5S sequences are identical and both are derived from *S. solfataricus*. The *S. acidocaldarius* 5S sequence has been published more recently along with a brief documentation of the strain misidentification problem [P. Durovic, U. Kutay, C. Schleper, P. P. Dennis, *J. Bacteriol.* **176**, 514 (1994)].
14. B. E. H. Maden, M. E. Corbett, P. A. Heeney, K. Pugh, P. M. Ajuh, *Biochimie* **77**, 22 (1995). This assay is not able to identify unambiguously all ribose methylations, presumably because of interference from other neighboring modifications (e.g., base methylations) and strong secondary structure features. Cases of false negatives have also been observed in which no pause was detected at sites of known ribose methylation. For unexplained reasons, we experienced a far lower primer extension success rate with archaeal rRNA than previously with yeast rRNA.
15. S. Steinberg, A. Misch, M. Sprinzl, *Nucleic Acids Res.* **21**, 3011 (1993).
16. The search algorithm and general snoRNA gene model remained as originally described (3), although yeast/human snoRNA training data were replaced by *S. acidocaldarius* training data. Alignments of box features (C, D', and D) from *S. acidocaldarius* sRNAs sR1 to sR17 (Table 1) were used to create log odds weight matrices reflecting the frequency of each nucleotide at each position in each box feature. The lengths of the rRNA complementary region and the gaps between box features were scored with binned length distributions.

Overall, training data for the nucleotide content of the box features did not change substantially between the yeast/human and archaeal models, but the distribution of lengths between features did vary; archaeal sRNAs appear to be much more compact than those in eukaryotes, and the rRNA complementary regions are shorter, commonly 8 to 11 nt long compared with 10 to 14 nt complementarities most often found in *S. cerevisiae* snoRNAs. We used final snoRNA scores to rank candidates within each genome and inspected hits manually by descending score. Hits that completely overlapped >600 nt open reading frames called by Glimmer 1.04 [S. Salzberg, A. Delcher, S. Kasif, O. White, *Nucleic Acids Res.* **26**, 544 (1998)] were discarded. No absolute score cutoff was used because each species' candidates matched the *S. acidocaldarius*-trained model to a different degree, and we had no estimate of the total number of genes to be found or the variability of sequence features for each different species.

17. Two-thirds of the *S. solfataricus* genome was completed at the time of our searches. The Web sites for accessing the archaeal genomes are as follows: *S. solfataricus*, [niji.imb.nrc.ca/sulfolobus/](http://niji.imb.nrc.ca/sulfolobus/); *M. jannaschii* and *A. fulgidus*, [www.tigr.org/tdb/](http://www.tigr.org/tdb/); *A. pernix*, [www.mild.nite.go.jp/APEK1/](http://www.mild.nite.go.jp/APEK1/); *M. thermoautotrophicum*, [www.biosci.ohio-state.edu/~genomes/mthermo/](http://www.biosci.ohio-state.edu/~genomes/mthermo/); *P. abyssi*, [www.genoscope.cns.fr/Pab/](http://www.genoscope.cns.fr/Pab/); *P. horikoshii*, [www.bio.nite.go.jp/ot3db\\_index.html](http://www.bio.nite.go.jp/ot3db_index.html); and *P. furiosus*, [www.genome.utah.edu/sequence.html](http://www.genome.utah.edu/sequence.html). We gratefully acknowledge the *Sulfolobus solfataricus* P2 Genome Project ([niji.imb.nrc.ca/sulhome](http://niji.imb.nrc.ca/sulhome)), Genoscope ([www.genoscope.cns.fr](http://www.genoscope.cns.fr)), and the Utah Genome Center, Department of Human Genetics, University of Utah ([www.genome.utah.edu](http://www.genome.utah.edu)) for access to unpublished genome sequence data.
18. Supplemental information is available at [www.sciencemag.org/feature/data/1047007.shl](http://www.sciencemag.org/feature/data/1047007.shl). All newly identified archaeal snoRNAs and annotation are also available at [rna.wustl.edu/snoRNAdb/](http://rna.wustl.edu/snoRNAdb/).
19. R. Gupta, *J. Biol. Chem.* **259**, 9461 (1984).
20. Numerous candidate sRNAs that had one or more

imperfect features were found in the genomes of the *S. solfataricus*, *M. jannaschii*, *A. fulgidus*, *A. pernix*, and *M. thermoautotrophicum*, but in the absence of identified ribose methylation sites or other confirmatory information, their authenticity remains uncertain. In particular, no strong candidates were identified within *M. thermoautotrophicum*, although we believe at least some of the search hits are legitimate (broader sRNA training data and/or the opportunity to test several dozen candidates experimentally are needed).

21. For each *Pyrococcus* sRNA homology group, the sequence identity for end-to-end alignments of interspecies members was 80 to 98%.
22. J. D. Thompson, D. G. Higgins, T. J. Gibson, *Nucleic Acids Res.* **22**, 4673 (1994). For our alignments, we anchored the 5' ends of the 16S rRNA with the conserved sequence GGUUGAUCCU; this block occupies positions 16 to 25 in all the 16S sequences in our alignment. The 235 sequences were anchored with the conserved sequence GGAUGGCCUCG. In the respective 235 sequences in our alignment, this block occupies positions 21 to 30 in *Afu*, 22 to 31 in *Mja*, 33 to 42 in *Pho*, 20 to 29 in *Ape*, 28 to 37 in *Sso*, and 33 to 42 in *Sac*.
23. K. T. Tycowski, Z.-H. You, P. G. Graham, J. A. Steitz, *Mol. Cell* **2**, 629 (1998); T. Pederson, *Nucleic Acids Res.* **26**, 3871 (1998).
24. C. J. Daniels, personal communication; D. W. Armbruster and C. J. Daniels, *J. Biol. Chem.* **272**, 19758 (1997).
25. We thank J. W. Brown for generously providing *M. jannaschii* total RNA used in verifying sRNA predictions. Work in P.P.D.'s laboratory was supported by the Medical Research Council of Canada, grant MT6340; work in S.R.E.'s laboratory was supported by NIH National Human Genome Research Institute grant HG01363.

11 November 1999; accepted 24 February 2000

## Transport of Peptide–MHC Class II Complexes in Developing Dendritic Cells

Shannon J. Turley,<sup>1</sup> Kayo Inaba,<sup>2</sup> Wendy S. Garrett,<sup>1</sup> Melanie Ebersold,<sup>1</sup> Julia Unternaehrer,<sup>1</sup> Ralph M. Steinman,<sup>3</sup> Ira Mellman<sup>1\*</sup>

Major histocompatibility complex class II (MHC II) molecules capture peptides within the endocytic pathway to generate T cell receptor (TCR) ligands. Immature dendritic cells (DCs) sequester intact antigens in lysosomes, processing and converting antigens into peptide–MHC II complexes upon induction of DC maturation. The complexes then accumulate in distinctive, nonlysosomal MHC II<sup>+</sup> vesicles that appear to migrate to the cell surface. Although the vesicles exclude soluble lysosomal contents and antigen-processing machinery, many contain MHC I and B7 costimulatory molecules. After arrival at the cell surface, the MHC and costimulatory molecules remain clustered. Thus, transport of peptide–MHC II complexes by DCs not only accomplishes transfer from late endocytic compartments to the plasma membrane, but does so in a manner that selectively concentrates TCR ligands and costimulatory molecules for T cell contact.

A pivotal step in the initiation of T cell immunity is the presentation of antigenic peptides by MHC products expressed on DCs. In general, MHC II molecules bind peptides formed in endocytic organelles (1). In antigen-presenting cells (APCs) such as

B lymphocytes, MHC II accumulates in late endosomal and lysosomal compartments (collectively termed MIICs) together with other components required for antigen processing. These include the invariant (Ii) chain that targets MHC II from the Golgi to

## REPORTS

endocytic organelles, H-2M that helps peptides gain access to MHC II, and proteases, notably cathepsin S (2). MIICs are thus viewed as a primary site for peptide-MHC II complex formation. It is not clear, however, how peptide-MHC II complexes formed in lysosomes are transferred to the surface because lysosome-to-plasma membrane transport, although it can occur, is

inefficient in most cell types (3, 4).

Nonlysosomal MHC II<sup>+</sup> compartments termed CIIVs have also been described (5). CIIVs are particularly abundant in DCs that are at an intermediate stage of maturation (6). The relative functions of MIICs and CIIVs have thus far been difficult to analyze directly, particularly in the case of CIIVs, which are a minor population of MHC II<sup>+</sup> structures in B cells and exist only transiently in DCs.

Our recent results suggested that the formation of peptide-MHC II complexes in DCs is tightly controlled (7). In immature DCs, corresponding to those found in peripheral tissues, neither peptides nor proteins were converted to peptide-MHC II complexes until after the receipt of a maturation stimulus [e.g., lipopolysaccharide (LPS)]. Shortly thereafter, the complexes first appeared in lysosomal compartments and subsequently at

the plasma membrane (7). Because DC maturation is characterized by a dramatic up-regulation in surface expression of MHC II and costimulatory molecules required for T cell stimulation (6, 8), we investigated whether and how peptide-MHC complexes formed in lysosomes reached the cell surface.

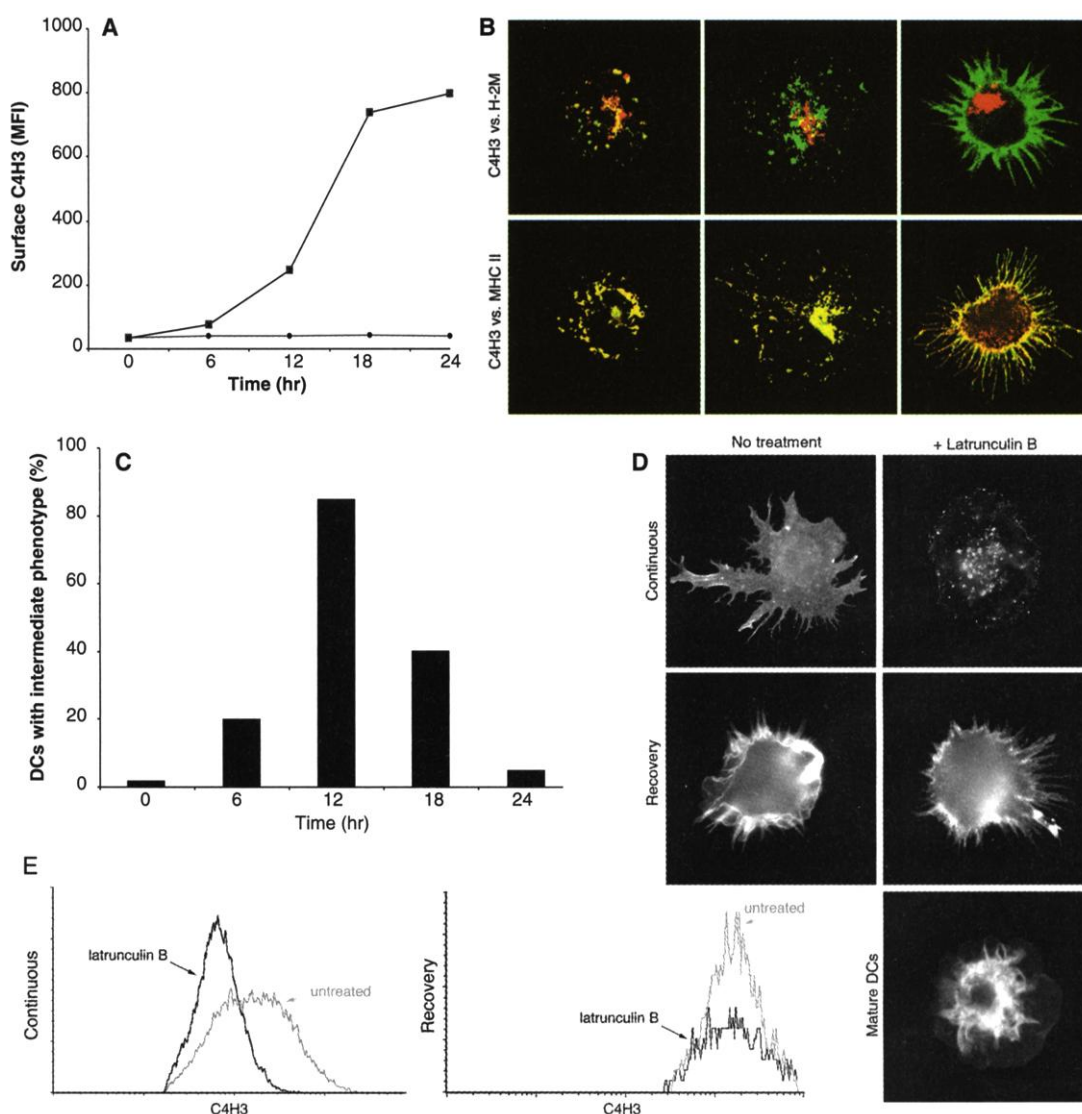
As in our previous study (7), we used a monoclonal antibody (C4H3) that detects hen egg lysozyme (HEL) peptide 46-61 bound to I-A<sup>k</sup> to monitor the formation and fate of a specific peptide-MHC II complex (9). Exposure of immature DCs to HEL generated C4H3-reactive complexes only when the cells were also exposed to a maturation stimulus such as LPS (7).

To determine the kinetics of peptide-MHC II complex formation and transport, immature DCs were pulsed with HEL with or without LPS for 1 hour, washed, and chased

<sup>1</sup>Department of Cell Biology and Section of Immunobiology, Ludwig Institute for Cancer Research, Yale University School of Medicine, 333 Cedar Street, Post Office Box 208002, New Haven, CT 06520-8002, USA. <sup>2</sup>Laboratory of Immunobiology, Graduate School of Biostudies, Kyoto University, Kyoto 606-8502, Japan. <sup>3</sup>Laboratory of Cellular Immunology and Physiology, Rockefeller University, 1230 York Avenue, New York, NY 10021-6399, USA.

\*To whom correspondence should be addressed. E-mail: ira.mellman@yale.edu

**Fig. 1.** Peptide-MHC II complexes accumulate in CIIVs. **(A)** Immature CBA/J DCs were pulsed with LPS-depleted HEL (3 mg/ml) or HEL (3 mg/ml) plus LPS (5 ng/ml) for 1 hour, gently washed, chased in HEL- and LPS-free media, and assayed every 6 hours for HEL peptide-MHC II complexes [y axis displays the mean fluorescence intensity (MFI) of C4H3 reactivity] by flow cytometry. The x axis displays the time in culture after addition of antigen. **(B)** Immature I-A<sup>k+</sup> DCs treated with HEL plus LPS [as in (A)] were harvested after 4 hours (left), 9 hours (middle), or 22 hours (right) and processed for ICM. Optically merged images display DCs double-labeled with antibodies specific for HEL peptide-MHC II complexes (upper panels, green) and H-2M (upper panels, red) or HEL peptide-MHC II complexes (lower panels, green) and total MHC II (lower panels, red). **(C)** Using phenotypic criteria established previously (5), the intermediate DC frequency was determined at various times during HEL pulse-chase assays [as in (A)]. Data are representative of more than 10 experiments. **(D)** The localization of HEL peptide-MHC II complexes was monitored by ICM in I-A<sup>k+</sup> DCs cultured in the presence (right) or absence (left) of LatB (0.4 μg/ml) with C4H3. Immature DCs were pulsed with HEL (3 mg/ml) for 1 to 3 hours and washed. DCs were then either treated continuously with LatB for 12 to 36 hours (upper panels, Continuous), treated for 12 hours with LatB, and then recultured in the absence of drug for an additional 12 hours (middle



panels, Recovery), or induced to mature with LPS. Mature DCs were treated with LatB for 2 hours (lower panel, Mature DCs). **(E)** As in (D), but DCs were processed for flow cytometry. C4H3 reactivity on LatB-treated (black) and untreated control (gray) I-E<sup>+</sup> DCs is shown.

## REPORTS

for various times (10). As expected, flow cytometry demonstrated that C4H3-reactive complexes did not appear at the plasma membrane unless LPS was included with the HEL (Fig. 1A) (7, 11). Nevertheless, there was an appreciable lag (~12 hours) before HEL peptide–MHC II complexes were detected. Surface C4H3 complexes reached a plateau at ~18 hours.

When LPS-treated DCs were examined by immunofluorescence confocal microscopy (ICM), intracellular C4H3 staining was evident within 4 hours of chase (12). Most of the C4H3<sup>+</sup> cells exhibited the immature DC phenotype with abundant HEL peptide–MHC II complexes in H-2M<sup>+</sup>/LAMP<sup>+</sup> lysosomal compartments (MIICs) (Fig. 1B, upper left panel). C4H3 staining colocalized with total MHC II (detected with an antibody to the  $\beta$  chain of I-A) in immature DCs (Fig. 1B, lower left panel).

At 9 hours of chase, intracellular staining was abundant but C4H3-reactive HEL peptide–MHC II complexes were localized to the population of nonlysosomal, peripheral vesi-

cles previously designated as CIIV (Fig. 1B, upper middle panel) (5). Unlike MHC II<sup>+</sup> structures labeled at earlier time points, CIIVs were negative for the lysosomal membrane markers LAMP and H-2M. C4H3 staining in CIIVs again colocalized with total MHC II (Fig. 1B, lower middle panel), indicating that these DCs were of the “intermediate” maturational phenotype (6).

After 22 hours of chase, most of the cells exhibited surface C4H3 staining with relatively little intracellular staining (Fig. 1B, upper right panel; total MHC II in lower right panel). Quantitation of random images from several experiments demonstrated that the incidence of the CIIV-containing intermediate DCs reached a maximum at ~12 hours (Fig. 1C), just as HEL peptide–MHC II complexes began to accumulate at the plasma membrane. Thus, CIIVs appeared to be intermediates in the transfer of peptide–MHC II complexes from lysosomes to the plasma membrane.

We next screened for agents that inhibited CIIV transport. Depolymerization of micro-

tubules with nocodazole was without effect, but treatment with the actin antagonist Latrunculin B (LatB) affected CIIV translocation and C4H3 delivery (13).

Immature DCs were pulsed with HEL and LPS for 1 to 3 hours, washed, and cultured in the presence of 0.4  $\mu$ g/ml LatB (13). Cultures treated with LatB accumulated cells with C4H3-reactive CIIVs relative to untreated controls for as long as 12 to 36 hours of chase (Fig. 1D, upper panels). The effect did not cause an appreciable decrease in total C4H3 reactivity (measured by intracellular staining with fluorescence-activated cell sorting) and, moreover, it was reversible; subsequent incubation for 12 hours in the absence of LatB resulted in the disappearance of CIIVs and the appearance of C4H3-reactive complexes on the cell surface (Fig. 1D, middle panels). Treatment of mature DCs with LatB did not cause the accumulation of CIIV-like vesicles (Fig. 1D, bottom panel), indicating that the drug did not induce endocytosis of surface MHC II.

When the same cells were analyzed for surface C4H3-reactive complexes by flow

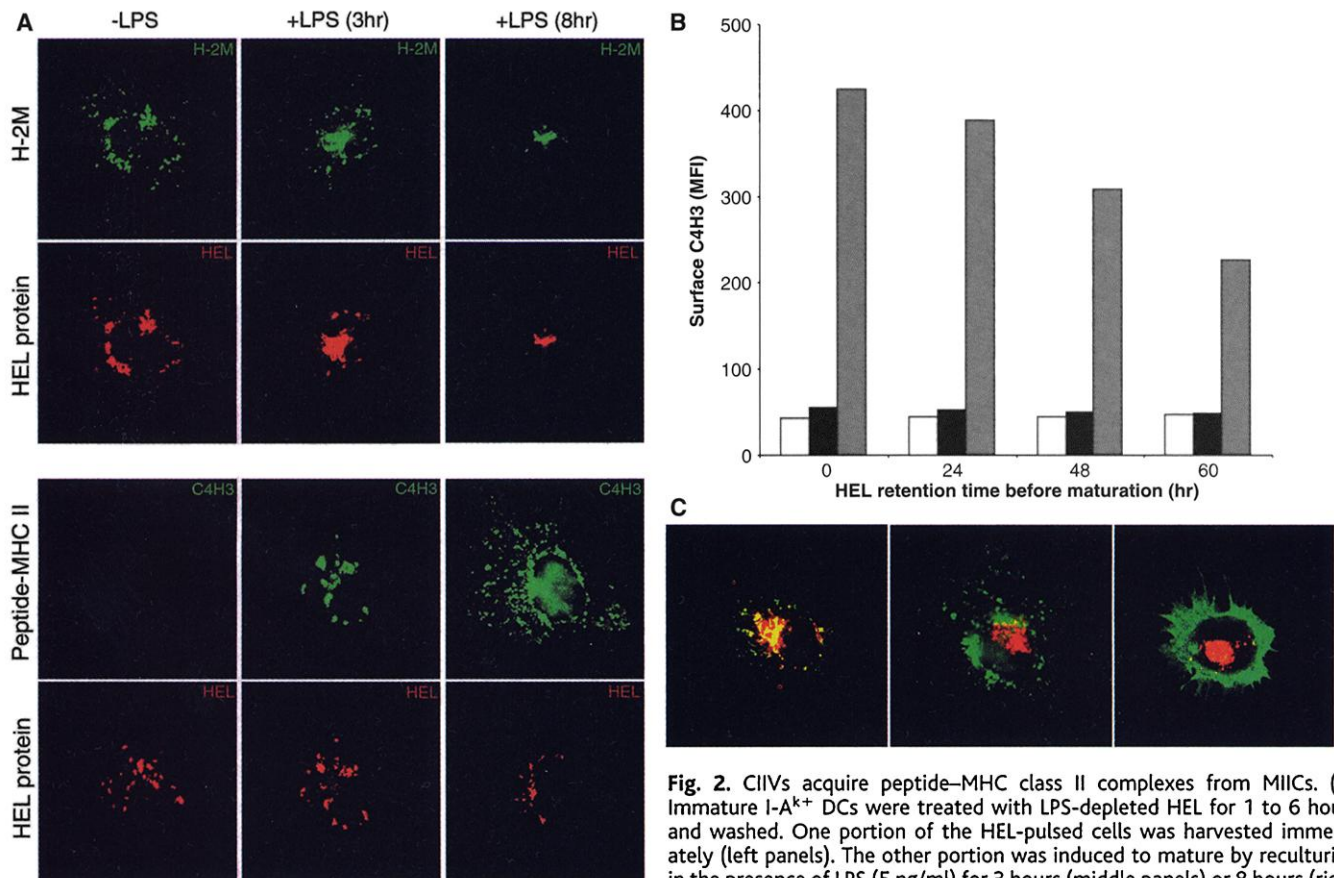


**Fig. 2.** CIIVs acquire peptide–MHC class II complexes from MIICs. (A) Immature I-A<sup>k+</sup> DCs were treated with LPS-depleted HEL for 1 to 6 hours and washed. One portion of the HEL-pulsed cells was harvested immediately (left panels). The other portion was induced to mature by reculturing in the presence of LPS (5 ng/ml) for 3 hours (middle panels) or 8 hours (right panels). Both sets of cells were processed for ICM. Cells were double-labeled

with antibodies specific for H-2M (upper panels, green) and HEL protein (lower panels, red). (B) Immature I-A<sup>k+</sup> DCs were pulsed with LPS-depleted HEL (3 mg/ml) for 1 hour, washed, chased in HEL-free media for the time indicated on the x axis, and then treated with LPS for 18 hours. Conditions include DCs treated with no HEL and no LPS (open bars), DCs pulsed with LPS-depleted HEL (black bars), or DCs pulsed with LPS-depleted HEL and then LPS after the chase (shaded bars). DCs were processed for flow cytometry to quantitate surface expression of HEL peptide–MHC II complexes. (C) Immature I-A<sup>k+</sup> DCs were pulsed with LPS-depleted HEL (3 mg/ml) for 1 hour, washed, chased in HEL-free media for 24 hours, and then exposed to LPS for 3 hours (left), 8 hours (middle), or 22 hours (right). To analyze the localization of C4H3, we processed cells for ICM. Optically merged images of DCs stained for C4H3 (green) and H-2M (red).

## REPORTS

cytometry, LatB treatment was found to cause a partial but substantial (up to 50%) decrease in C4H3 reactivity (Fig. 1E, left panel) (11). A second MHC II product that is not C4H3-reactive, I-E<sup>k</sup>, was reduced to the same extent, as would be expected if CIIVs were responsible for delivering all MHC II molecules to the surface. Upon reculture in the absence of LatB, surface expression of both C4H3-reactive (I-A<sup>k</sup>) and nonreactive (I-E<sup>k</sup>) complexes were restored (Fig. 1E, right panel). Thus, the LatB-induced decrease in plasma membrane MHC II correlated with the accumulation of CIIVs, supporting the possibility that CIIVs are intermediates in the delivery of at least a portion of the MHC II complexes to the cell surface.

We next examined whether HEL internalized before, rather than concomitant with, LPS treatment could be used to generate C4H3<sup>+</sup> complexes that would then be delivered to the cell surface. When immature DCs were incubated with LPS-free HEL for 1 to 6 hours, HEL protein was found to accumulate in H-2M<sup>+</sup> lysosomes (Fig. 2A, upper left panels). As expected (7), the immature cells were unable to convert the HEL protein into C4H3-reactive complexes (Fig. 2A, lower left panels).

When the cells were then treated with LPS for 3 hours to initiate maturation (Fig. 2A, center panels), the internalized HEL protein remained in lysosomal structures that began to cluster in the perinuclear cytoplasm (upper center panels). However, the antigen-containing lysosomes then became strongly positive for the C4H3 epitope, indicating the formation of immunogenic HEL peptide-MHC II complexes (lower center panels).

Within 8 hours of the LPS pulse, HEL protein remained in the increasingly perinuclear lysosomal structures (Fig. 2A, upper right panels). In contrast, the C4H3-reactive peptide-MHC II complexes became largely segregated from the HEL and were found in CIIVs (lower right panels). Thus, the appearance of CIIV was accompanied by the sorting of peptide-MHC II complexes from lysosomal membrane proteins (LAMP, H-2M) and contents (HEL).

DCs converted HEL into C4H3<sup>+</sup> peptide-MHC II complexes even when the HEL was internalized long before the receipt of a maturation stimulus. Immature DCs were pulsed with LPS-free HEL (7, 10) for 1 hour, washed, and then chased for up to 3 days in HEL-free media. The cells were only then treated with LPS to initiate maturation. The internalized HEL was not converted into C4H3-reactive complexes for at least 60 hours unless the cells were treated with LPS at the end of the chase (Fig. 2B). Thus, immature DCs can retain previously internalized HEL for several days before converting it to immunogenic complexes. Even after extended chase periods, LPS treatment triggered the appearance 3 to 4 hours later of C4H3<sup>+</sup> HEL peptide-MHC II in lysosomal compartments (Fig. 2C, left), followed by the segregation of the peptide-MHC II into nonlysosomal CIIV (center), and subsequent appearance on the plasma membrane in mature DCs (right).

Despite their differences in function, lysosomal MIICs and CIIVs were similar morphologically, as indicated by immunoelectron microscopy (IEM) (14). Immature DCs contained abundant LAMP<sup>+</sup> and MHC II<sup>+</sup> structures (MIICs) that, as expected, displayed

internal membrane vesicles or lamellae (15) (Fig. 3, A and B). Similar structures were observed in CIIV-containing intermediate DCs, except that the MHC II<sup>+</sup> elements lacked the lysosomal marker LAMP-2 (Fig. 3, C and D). The structural homology between MIICs and CIIVs suggests that CIIVs may arise directly from MHC II<sup>+</sup> lysosomes. If true, CIIVs might form as a result of a sorting event that selectively includes peptide-MHC II complexes while excluding lysosomal residents. Indeed, we occasionally observed "hybrid" MHC II<sup>+</sup> vesicles in which part of the vesicle contained LAMP-2 and part did not (Fig. 3E).

Regardless of the precise pathway of origin of CIIV, their selective accumulation of peptide-MHC II complexes suggested that they might include other molecules relevant to antigen presentation. Indeed, CIIVs in DCs from both mice and rats contained MHC I as well as the B7-2 (CD86) costimulatory molecule. In intermediate-stage DCs, MHC I and B7-2 exhibited punctate intracellular staining distinct from LAMP<sup>+</sup> lysosomes (Fig. 4A, top panels). In double-labeling experiments, MHC I colocalized extensively with MHC II, with B7-2 and MHC II colocalizing to a somewhat lesser extent (Fig. 4A). That B7-2 and MHC II could be found in the same structures was confirmed by IEM (Fig. 4B).

In a subset of DCs that express the glycosylphosphatidyl inositol-anchored protein Thy-1, this marker was also found in CIIVs, suggesting that these structures may contain glycosphingolipid rafts (16). CIIVs were negative, however, for LFA-1, transferrin receptor, and Fc receptor (FcR $\gamma$ II). Thus, although

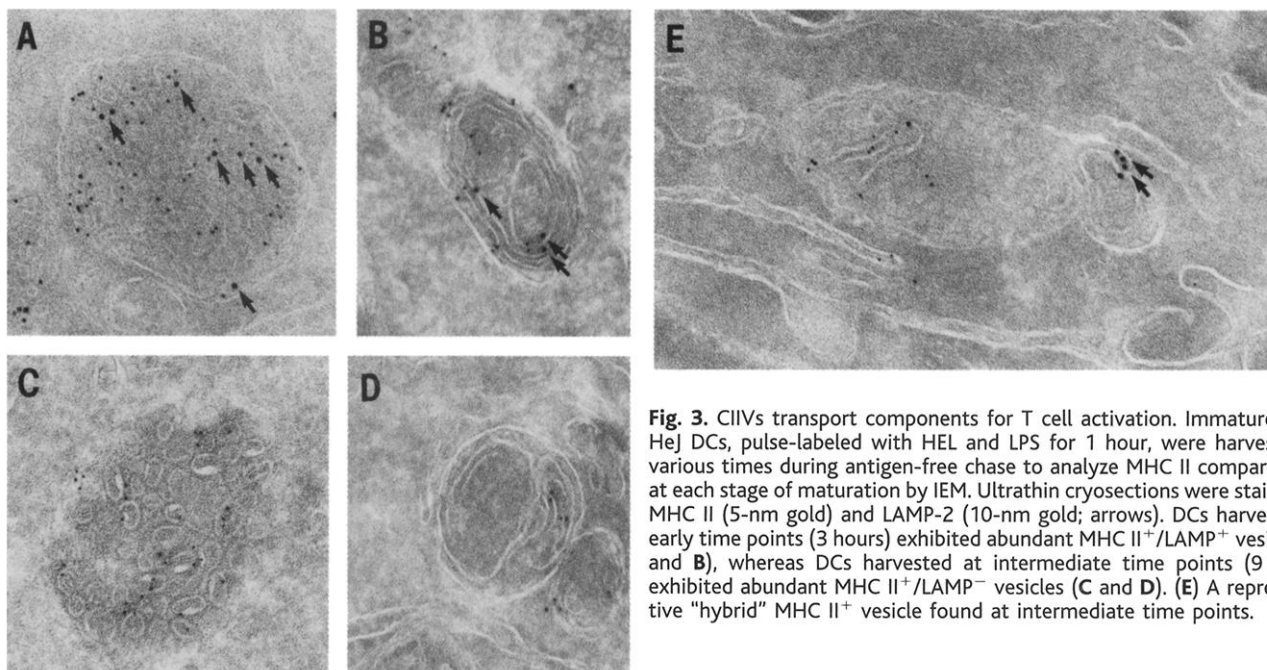


**Fig. 3.** CIIVs transport components for T cell activation. Immature C3H/HeJ DCs, pulse-labeled with HEL and LPS for 1 hour, were harvested at various times during antigen-free chase to analyze MHC II compartments at each stage of maturation by IEM. Ultrathin cryosections were stained for MHC II (5-nm gold) and LAMP-2 (10-nm gold; arrows). DCs harvested at early time points (3 hours) exhibited abundant MHC II<sup>+</sup>/LAMP<sup>+</sup> vesicles (A and B), whereas DCs harvested at intermediate time points (9 hours) exhibited abundant MHC II<sup>+</sup>/LAMP<sup>-</sup> vesicles (C and D). (E) A representative "hybrid" MHC II<sup>+</sup> vesicle found at intermediate time points.

## REPORTS

some compositional heterogeneity was observed, CIIVs selectively accumulate T cell receptor (TCR) ligands (MHC I and II) together with at least one costimulatory molecule required for T cell activation (B7-2).

The CIIVs were not formed by endocytosis of MHC II from the plasma membrane. When intermediate DCs were incubated with monoclonal antibody to MHC II for various periods of time, internalized antibody accumulated in lysosomal vesicles distinct from the MHC II<sup>+</sup> CIIVs (Fig. 4A, middle right panel). Similar results were obtained with markers of fluid endocytosis whether internalized before or after a maturation stimulus (17). Indeed, most CIIV-containing DCs were unable to internalize the antibody or other markers at all, because endocytosis is rapidly down-regulated upon receipt of a maturation stimulus (17).

Despite the considerable degree of colocalization between MHC II, MHC I, and B7-2 in CIIVs of intermediate DCs, these markers exhibited distinct distributions in immature DCs. Although MHC II molecules were found in LAMP<sup>+</sup> lysosomes, both MHC I and B7-2 exhibited a reticular, endoplasmic reticulum (ER)-like pattern largely separate from MHC II (Fig. 4A, lower panels). Conceivably, immature

DCs retain MHC I and B7-2 in the ER, to be exported upon receipt of a maturation stimulus. Disappearance from the ER in mature cells correlates with a transient increase in the synthesis of both markers (18, 19).

Late in the intermediate stage of DC development, MHC II, MHC I, C4H3-reactive complexes, and B7-2 begin to appear at the cell surface. Even after arrival at the plasma membrane, these markers continued to exhibit a punctate distribution (Fig. 4C). MHC II, B7-2, and peptide-MHC II complexes continued to colocalize at least in part with one another, a distribution that persisted for long periods into the mature stage of DC development (Fig. 4C).

Not all plasma membrane components were contained within the DC surface clusters. For example, in both intermediate and mature DCs, LFA-1 (CD18) and ICAM-1, not present in CIIVs, were diffusely distributed on the plasma membrane (Fig. 4C). Additionally, the clustered distribution of surface MHC II was found on DCs but not B cells expressing similar concentrations of MHC II (18). The difference in MHC II distribution on B cells versus DCs was also supported by preliminary IEM on cells first

fixed with glutaraldehyde. Thus, clustering of MHC II on the surface of DCs seems to reflect a cell type-limited rather than an antibody-dependent event.

Our results suggest that DCs use a distinctive population of nonlysosomal vesicles, CIIVs, to transfer peptide-MHC complexes from their site of formation in lysosomal compartments to the cell surface. These vesicles are notable for their ability to selectively accumulate not only peptide-MHC II but also MHC I and B7-2. It is as yet unclear how CIIVs form or if they serve as secretory vesicles that directly deliver their contents to the cell surface. Conceivably, they may communicate with the plasma membrane and their originating compartments through as yet undetected populations of transport vesicles. If CIIVs were to fuse directly with the plasma membrane, however, they might serve as the DC equivalent of neuronal synaptic vesicles, delivering TCR ligands and costimulatory molecules to facilitate the formation of an "immunological synapse" between the DC and T cells (20).

The cell biological mechanisms underlying the formation and fate of CIIVs represent critical unknowns. DCs may regulate entry into CIIV not only by controlling transport of

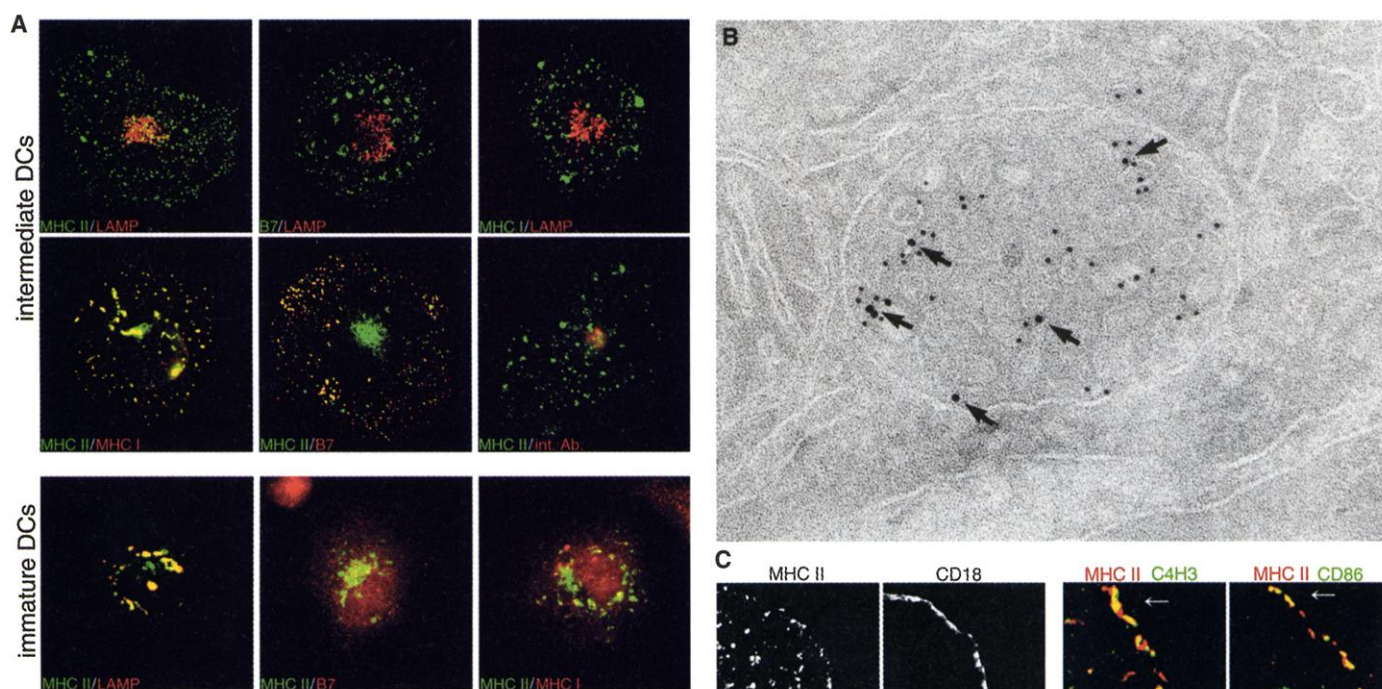


**Fig. 4.** MHC-B7 clusters at the DC plasma membrane. (A) DCs were harvested at the immature (bottom row) and intermediate stages (top and middle rows) and processed for ICM or IEM (B). One set of intermediate DCs was fed anti-MHC II for 2 hours (middle right panel). Cells were stained with antibodies specific for MHC II, LAMP-2, B7, MHC I, or anti-MHC II or with a CTLA-4-Ig fusion protein. ICM panels (A) contain optically merged, double-labeled DCs. The IEM panel (B) shows representative MHC II (5-nm gold) and B7-2 (10-nm gold, arrows) labeling in intermediate-stage DCs. (C). HEL-treated DCs were harvested late in the intermediate stage (10 to 12 hours after maturation induction) and processed for ICM. Cells were single-labeled for MHC II (first panel) and CD18 (second panel) and double-labeled for total MHC II (red) and HEL-peptide MHC II complexes (third panel, green) and total MHC II (red) and B7-2 (fourth panel, green).

MHC II from lysosomes but also by regulating the exit of MHC I from the ER. In addition, CIIVs are probably not the only factor responsible for the increase in surface MHC II transport upon DC maturation. For example, DCs regulate the post-Golgi transport of newly synthesized MHC II molecules to lysosomes versus the plasma membrane by controlling both cathepsin S-mediated proteolysis of Ii chain and endocytosis of MHC II  $\alpha\beta$  dimers from the cell surface (6, 20). CIIVs appear to permit the recovery of MHC II synthesized before maturation and thus delivered to lysosomes.

DCs are perhaps the most potent of all APCs, being unsurpassed in their ability to stimulate immunologically naïve T cells (8). The features described here may contribute to their efficiency in several ways. First, the coupling of CIIV formation with the onset of DC maturation might explain how DCs sequester antigen in peripheral tissues for display to lymphoid organs, often days later. This strategy would enhance immune surveillance and maintenance of T cell memory. Second, the ability of MHC II and B7 molecules to cluster on the plasma membrane suggests that they are organized in a polyvalent configuration that may help to activate a quiescent T cell. In contrast, the recently described ability of T cells to mediate clustering of MHC and costimulatory molecules (20, 21) may serve to sustain rather than initiate an immune response.

References and Notes

1. C. Watts, *Annu. Rev. Immunol.* **15**, 821 (1997).
2. P. Cresswell, *Annu. Rev. Immunol.* **12**, 259 (1994); H. Chapman, *Curr. Opin. Immunol.* **10**, 93 (1998).
3. S. Kornfeld and I. Mellman, *Annu. Rev. Cell Biol.* **5**, 483 (1989).
4. J. Stinchcombe and G. M. Griffiths, *J. Cell Biol.* **147**, 1 (1999); R. Wubbolts et al., *J. Cell Biol.* **135**, 611 (1996); G. Raposo et al., *J. Exp. Med.* **183**, 1161 (1996).
5. S. Amigorena, J. R. Drake, P. Webster, I. Mellman, *Nature* **369**, 113 (1994).
6. P. Pierre et al., *Nature* **388**, 787 (1997); M. Talmor et al., *Eur. J. Immunol.* **28**, 811 (1998).
7. K. Inaba et al., *J. Exp. Med.* **191**, 927 (2000).
8. J. Banachereau and R. M. Steinman, *Nature* **392**, 245 (1998); I. Mellman, S. Turley, R. M. Steinman, *Trends Cell Biol.* **8**, 231 (1998).
9. G. Zhong, C. Reis e Sousa, R. N. Germain, *Proc. Natl. Acad. Sci. U.S.A.* **94**, 13856 (1997).
10. DC cultures were generated as described (5, 22). Immature I-A<sup>k+</sup> DCs grown from C3H/HeN, C3H/HeJ, and CBA/J (Jackson Labs, Bar Harbor, ME) marrow suspensions were pulsed with HEL (1 to 3 mg/ml) with or without LPS (1 to 10 ng/ml, *E. coli* 0111.B4) for 1 to 3 hours, washed, and chased in HEL- and LPS-free media. Similar results were obtained with DCs from each strain. DC cultures contained supernatant from mGM-CSF-expressing J558L cells (from A. Lanzavecchia, Basel Institute, Basel, Switzerland). LPS was removed from HEL (Sigma) with Kuttasuclean adsorbent (Maruha Corporation, Ibaraki, Japan). Maturation stimuli included LPS, CD40L, tumor necrosis factor- $\alpha$ , or replating (22).
11. DCs were fixed with 4% (wt/vol) paraformaldehyde and washed in phosphate-buffered saline. Cells were incubated with monoclonal antibodies (mAbs) on ice as described (23). The rat mAb C4H3 was provided by R. Germain (NIH, Bethesda, MD). C4H3 was purified on protein A-Sepharose and biotinylated. Cells were labeled with biotin-conjugated mAbs (Pharmingen) to I-E<sup>k</sup> (14-4-45) or I-A<sup>k</sup> (10-2.16) and fluorescein

isothiocyanate (FITC)-conjugated mAb to CD86 (GL1). Isotype controls were purchased from Pharmingen. Biotinylated mAbs were detected with streptavidin-phycoerythrin. Fluorescence analysis was done with a FACSCalibur and CellQuest software.

12. For ICM, DCs were adhered to Alcian blue-coated glass coverslips for 20 min at 37°C in serum-free media. Cell were fixed in 4% (wt/vol) PFA and permeabilized (for intracellular staining) in 0.05% saponin, 10 mM Hepes (pH 7.4), 10 mM glycine (pH 8.0), and 10% goat serum in RPMI 1640. Antibody incubations were done as described (6). Purified C4H3 was used for microscopy. To detect HEL, we used the mouse mAb 1B12, provided by P. Allen (Washington University, St. Louis, MO). Rabbit anti-H-2M (ULM) and rabbit anti-mouse I-A (RIV) have been described elsewhere (6). Hybridomas TIB126 (anti-MHC I), TIB99 (anti-Thy1.2), and TIB93 (anti-I-Ak) were obtained from American Type Culture Collection. Rabbit anti-CD18 was a gift from P. Blier (Boehringer Ingelheim, CT). Several mouse anti-rat mAbs were the gift of J. P. Soullilou (University of Nantes, Nantes, France), including OX-18 (anti-MHC I), anti-Thy1.1, and OX-6 (anti-MHC II). Rat B7 was detected with a CTLA-4-human IgG fusion protein (a gift of P. Linsley, Bristol Meyers Squibb) in combination with a FITC-conjugated horse anti-human IgG. Mouse B7-2 was detected with GL1. Rat lysosomes were stained with rabbit Igp120 antiserum (24). Irrelevant isotype-matched mAbs, preimmune rabbit serum, or normal human serum were used as negative controls in all experiments. Coverslips were mounted in Mowiol with DABCO (Calbiochem, La Jolla, CA), and fluorescence was analyzed with conventional and confocal (0.5- to 1.0- $\mu$ m optical sections) Zeiss microscopes.
13. DCs were treated with nocardazole (30  $\mu$ M, Sigma) or Latrunculin B (0.4 to 10  $\mu$ g/ml; Calbiochem, San Diego, CA) after the HEL pulse to allow internalization and immunogenic complex formation to occur.
14. DCs harvested at various times during the HEL pulse-

chase assay were fixed immediately with 4% PFA and 0.4% glutaraldehyde in 200 mM phosphate buffer. Cells were then processed for cryosectioning by embedding in 10% gelatin on ice. Blocks were saturated in 2.3 M sucrose overnight at 4°C. Ultrathin cryosections were retrieved with methylcellulose-sucrose and double-immunolabeled as described (25) with 5- and 10-nm gold particles. To identify MHCs and CIIVs, we used rat mAbs LAMP-1, LAMP-2, GL-1, and C4H3 and the mouse mAb 10-2.16 against I-A<sup>k</sup>.

15. C. V. Harding and H. J. Geuze, *J. Cell Biol.* **119**, 531 (1992); M. J. Kleijmeer, V. M. Oorschot, H. J. Geuze, *J. Invest. Dermatol.* **103**, 516 (1994); M. J. Kleijmeer, S. Morkowski, J. M. Griffith, A. Y. Rudensky, H. J. Geuze, *J. Cell Biol.* **139**, 639 (1997).
16. K. Simons and E. Ikonen, *Nature* **387**, 569 (1997)
17. W. S. Garrett and I. Mellman, in preparation.
18. J. Unternaehrer and I. Mellman, in preparation.
19. P. Pierre and I. Mellman, *Cell* **93**, 1135 (1998); M. Cella et al., *Nature* **388**, 782 (1997); M. Rescigno et al., *Proc. Natl. Acad. Sci. U.S.A.* **95**, 5229 (1998).
20. A. Grakoui et al., *Science* **285**, 221 (1999).
21. C. R. Monks, B. A. Freiberg, H. Kupfer, N. Sciaky, A. Kupfer, *Nature* **395**, 82 (1998).
22. K. Inaba et al., *J. Exp. Med.* **176**, 1693 (1992).
23. K. Inaba et al., *J. Exp. Med.* **188**, 2163 (1998).
24. V. Lewis et al., *J. Cell Biol.* **100**, 1839 (1985).
25. J. W. Slot and H. J. Geuze, *Eur. J. Cell Biol.* **38**, 87 (1985).
26. We thank members of the Mellman, Steinman, and Inaba laboratories for valuable advice. Supported by grants from NIH (AI-34098 to I.M.), the National Institute of Allergy and Infectious Diseases (AI-13013 and AI-39672 to R.M.S.), and the Ministry of Education, Science and Culture of Japan (grants 08282104, 10153226, and 10044268 to K.I.). I.M. is a member of the Ludwig Institute for Cancer Research.

15 October 1999; accepted 15 February 2000

# On the Origin of Internal Structure of Word Forms

Peter F. MacNeilage<sup>1\*</sup> and Barbara L. Davis<sup>2</sup>

This study shows that a corpus of proto-word forms shares four sequential sound patterns with words of modern languages and the first words of infants. Three of the patterns involve intrasyllabic consonant-vowel (CV) co-occurrence: labial (lip) consonants with central vowels, coronal (tongue front) consonants with front vowels, and dorsal (tongue back) consonants with back vowels. The fourth pattern is an intersyllabic preference for initiating words with a labial consonant-vowel-coronal consonant sequence (LC). The CV effects may be primarily biomechanically motivated. The LC effect may be self-organizational, with multivariate causality. The findings support the hypothesis that these four patterns were basic to the origin of words.

The most basic unit of language is the word—the minimal stand-alone pairing of meaning and sound structure. But what is the nature of this pairing? Apart from those few words that are indubitably onomatopoeic, linguists consider the pairing to be primarily “arbitrary” (1)—that is, they believe that a word’s conceptual structure does not impose a particular sound structure

on its spoken form across languages. But if the conceptual structure, or meaning, of a word does not determine its sound pattern, what does? Oddly, scant attention has been paid to how the spoken forms of words originate. Are there determining factors inherent in the very production of sound structures of words, beyond their well-known tendency to alternate between consonants and vowels, thus forming syllables (e.g., “to-ma-to”)? We have addressed this question by first looking at speech-related behavior at its simplest: in infants’ babbling and in their first words.

We conducted statistical studies of the bab-

<sup>1</sup>Department of Psychology, <sup>2</sup>Department of Communication Sciences and Disorders, University of Texas, Austin, TX 78712, USA.

\*To whom correspondence should be addressed. E-mail: macneilage@psy.utexas.edu